Research Square

Preprints are preliminary reports that have not undergone peer review.
They should not be considered conclusive, used to inform clinical practice,
or referenced by the media as validated information.

Adaptive-Compression Hyperbolic-Tangent Algorithm for Robust Adaptive Filtering

Pucha Song
Chengdu University
Yulong Wang
Chengdu University
Zhengyan Luo
luozhengyan@cdu.edu.cn
Chengdu University

Research Article

Keywords: Adaptive filtering, Hyperbolic tangent function, Non-Gaussian noise, System identification, Steady-state performance

Posted Date: November 26th, 2026

DOI: https://doi.org/10.21203/rs.3.rs-11624560/v1

License: This work is licensed under a Creative Commons Attribution 4.0 International License.
Read Full License

Additional Declarations: No competing interests reported.

Adaptive-Compression Hyperbolic-Tangent Algorithm for Robust Adaptive Filtering

Pucha Song[1], Yulong Wang[1], Zhengyan Luo[1*]

[1]School of Electronic Information and Electrical Engineering, Chengdu University, Chengdu, 610106, China.

*Corresponding author(s). E-mail(s): luozhengyan@cdu.edu.cn;
Contributing authors: songpucha@cdu.edu.cn; wangyulong@cdu.edu.cn;

Abstract

To address the poor robustness and possible divergence of the conventional least mean square (LMS) algorithm under non-Gaussian and impulsive noise, this paper proposes an adaptive-compression hyperbolic-tangent (ACHT) algorithm for robust adaptive filtering. By introducing an error-dependent compression mechanism into the nonlinear argument of the hyperbolic-tangent function, the proposed method adaptively regulates the influence of large-amplitude errors while preserving a sensitive response in the small-error region. Based on the energy conservation relation, a steady-state performance analysis framework for ACHT is established, and theoretical expressions of the steady-state mean-square deviation (MSD) and excess mean-square error (EMSE) are derived to reveal the relationship between algorithm parameters and steady-state performance. Monte Carlo simulations are conducted to verify the consistency between the theoretical steady-state MSD and simulation results, investigate the influence of key parameters, and compare ACHT with representative robust adaptive filtering algorithms. Experiments under different measurement noise conditions demonstrate that ACHT achieves improved convergence performance and lower steady-state NMSD compared with representative robust adaptive filtering algorithms.

Keywords: Adaptive filtering, Hyperbolic tangent function, Non-Gaussian noise, System identification, Steady-state performance

1 Introduction

Adaptive filtering is a fundamental technique in signal processing and has been widely applied to system identification, noise suppression, and time-series prediction. Among classical adaptive algorithms, the least mean square (LMS) algorithm is particularly attractive because of its simple structure and ease of implementation. However, because LMS minimizes a mean-square error criterion, its performance can deteriorate substantially in non-Gaussian environments, especially in the presence of impulsive noise. Large-amplitude errors may dominate the gradient update, resulting in unstable adaptation and degraded convergence performance [1].

To enhance robustness against such disturbances, existing studies mainly focus on designing new cost functions, adjusting step-size strategies, and introducing additional adaptive mechanisms. Nonlinear transformations based on logarithmic or hyperbolic structures, together with correntropy-based criteria, have become important approaches for robust adaptive filtering [1–6].

Chen et al. introduced the generalized maximum correntropy criterion (GMCC) for robust adaptive filtering under non-Gaussian noise [2]. Huang et al. proposed the maximum versoria criterion (MVC) to reduce the influence of impulsive errors on adaptive weight updates [3]. Robust adaptive filters based on sigmoid cost functions were also developed [4]. Liu et al. proposed a least lncosh (Llncosh) algorithm, whose smooth functional form reduces the influence of abnormal data [5]. Wang et al. developed the logarithmic hyperbolic cosine adaptive filter (LHCAF) to improve the stability of conventional hyperbolic-cosine-based algorithms in the presence of large initial errors [6]. Meanwhile, variable-step-size strategies, correntropy-based combinations, and sparsity-aware constraints have been explored to further improve the robustness and adaptability of adaptive filters [7–10].

More recently, several robust adaptive algorithms with saturating nonlinearities have been investigated. Jia et al. analyzed the steady-state performance of the arctangent LMS (ATLMS) algorithm and demonstrated that the saturation property of the arctangent function can effectively suppress impulsive disturbances [11]. Abdelrhman et al. introduced a generalized robust logarithmic family (GRLF) framework to improve steady-state convergence and robustness under Gaussian and non-Gaussian impulsive noise [12]. Patel et al. proposed a generalized soft-root-sign (GSRS) function and corresponding adaptive filters, which suppress large-outlier-induced weight updates and reduce steady-state misadjustment [13]. Song et al. reconstructed the cost function using a hyperbolic-tangent framework and developed the hyperbolic tangent least mean square (HTLMS) algorithm, which alleviates the influence of gradient noise [14]. Subsequent studies have examined robust adaptive filtering in diffusion networks [15], quaternion-valued systems [16], and impulsive, colored, or heavy-tailed noise environments [17–19].

Although nonlinear error functions can reduce the influence of impulsive disturbances, their responses to errors of different magnitudes depend on the function form and parameter settings.

This paper proposes an adaptive-compression hyperbolic-tangent (ACHT) algorithm for robust adaptive filtering. The proposed algorithm introduces an error-dependent compression term into the argument of the hyperbolic tangent function to regulate the response to errors of different magnitudes. Based on an energy-conservation relation, approximate expressions for the steady-state mean-square deviation (MSD) and excess mean-square error (EMSE) are derived. Monte Carlo simulations are conducted to assess the theoretical predictions, investigate parameter sensitivity, and compare ACHT with representative robust adaptive filtering algorithms under different measurement-noise distributions.

2 Proposed Adaptive-Compression Hyperbolic-Tangent Algorithm

2.1 System Identification Model

Fig. 1 illustrates the system identification structure considered in this work. Let $\boldsymbol{x}_k$ and $\boldsymbol{w}_k$ denote the input vector and the adaptive filter weight vector, respectively. The adaptive filter aims to estimate the unknown system vector $\boldsymbol{w}^o$. The desired response of the unknown system is expressed as

$$d_k = \boldsymbol{x}_k^T \boldsymbol{w}^o + v_k \tag{1}$$

where $\boldsymbol{x}_k$ is an L-dimensional input vector, and v_k denotes the measurement noise. The output of the adaptive filter is

$$y_k = \boldsymbol{x}_k^T \boldsymbol{w}_k. \tag{2}$$

Accordingly, the error signal can be written as

$$\begin{aligned} e_k &= d_k - y_k \\ &= \boldsymbol{x}_k^T (\boldsymbol{w}^o - \boldsymbol{w}_k) + v_k. \end{aligned} \tag{3}$$

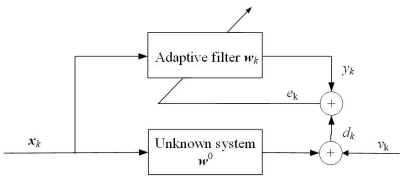

Fig. 1: System identification model.

2.2 Adaptive-Compression Hyperbolic-Tangent Algorithm

In the conventional LMS algorithm, large estimation errors lead to large weight updates, which may degrade performance under impulsive noise. To reduce the influence of such errors, the ACHT cost function is defined as

$$J(e_k) = \frac{1}{\lambda} \tanh\left(\lambda \frac{|e_k|^p}{1+\alpha|e_k|^{p-1}}\right) \tag{4}$$

where the parameters satisfy $p > 1$, $\alpha > 0$, and $\lambda > 0$. The parameter p controls the nonlinear growth behavior, α regulates the error-dependent compression strength, and λ determines the saturation characteristics.

Fig. 2 shows the effects of these parameters on the cost function. In each case, one parameter is varied while the other two are fixed. For the p curves, $\alpha = 0.03$ and $\lambda = 0.01$; for the α curves, $p = 2$ and $\lambda = 0.01$; and for the λ curves, $p = 2$ and $\alpha = 0.03$. The instantaneous term in (4) is used to obtain the plotted curves.

As shown in Fig. 2(a), increasing p makes the transition toward saturation sharper. In Fig. 2(b), a larger α slows the growth of the cost function without changing its saturation level. Fig. 2(c) shows that increasing λ lowers the saturation level, which is given by $1/\lambda$.

Using the stochastic gradient approach, the instantaneous gradient with respect to the weight vector is obtained as

$$\begin{aligned} \nabla_{\boldsymbol{w}} J(e_k) &= \frac{\partial J(e_k)}{\partial e_k} \frac{\partial e_k}{\partial \boldsymbol{w}_k} \\ &= -\varphi(e_k)\boldsymbol{x}_k \end{aligned} \tag{5}$$

where $\varphi(e_k)$ is the gradient of the cost function $J(e_k)$ with respect to the error e_k, defined as

$$\begin{aligned} \varphi(e_k) = \operatorname{sech}^2\left(\frac{\lambda|e_k|^p}{1+\alpha|e_k|^{p-1}}\right) \\ \cdot \frac{|e_k|^{p-2}e_k\left[p+\alpha|e_k|^{p-1}\right]}{\left(1+\alpha|e_k|^{p-1}\right)^2} \end{aligned} \tag{6}$$

where $\operatorname{sech}(\cdot)$ denotes the hyperbolic secant function. For $p > 1$, the derivative at $e_k = 0$ is defined by continuity as $\varphi(0) = 0$.

The effects of the three parameters on $\varphi(e_k)$ are plotted in Fig. 3. Fig. 3(a) shows that a larger p produces a higher gradient peak and a narrower response range. As α increases, the peak magnitude decreases, as shown in Fig. 3(b). In Fig. 3(c), increasing λ reduces the gradient magnitude and causes a faster decay at large error values.

The resulting ACHT weight update is given by

$$\boldsymbol{w}_{k+1} = \boldsymbol{w}_k + \mu\varphi(e_k)\boldsymbol{x}_k \tag{7}$$

where μ is the step size. For large error magnitudes, $\varphi(e_k)$ approaches zero, reducing the effect of impulsive disturbances on the weight update.

3 Performance Analysis

3.1 Steady-State Performance Analysis

To analyze the steady-state performance of the proposed ACHT algorithm, let $P = L$ denote the number of filter coefficients. The weight-error vector is defined as

$$\widetilde{\boldsymbol{w}}_k = \boldsymbol{w}^o - \boldsymbol{w}_k. \tag{8}$$

The a priori error is given by

$$e_{a,k} = \boldsymbol{x}_k^T \widetilde{\boldsymbol{w}}_k. \tag{9}$$

For the steady-state analysis, the measurement noise is assumed to be Gaussian, i.e., $v_k = \xi_k$. Equation (3) can then be written as

$$e_k = e_{a,k} + \xi_k \tag{10}$$

For analytical tractability, the following assumptions are adopted:

1. Noise assumption: $\xi_k \sim \mathcal{N}(0, \sigma_\xi^2)$ is i.i.d. and independent of $\boldsymbol{x}_k$.
2. Error independence: The a priori error $e_{a,k}$ is zero-mean and independent of ξ_k.
3. Input assumption: $\boldsymbol{x}_k$ is a zero-mean Gaussian input with covariance matrix $\boldsymbol{R} = \sigma_x^2 \boldsymbol{I}$.
4. Independence approximation: $\|\boldsymbol{x}_k\|^2$ and $\varphi^2(e_k)$ are asymptotically uncorrelated at steady state.

Here, σ_x^2 denotes the input variance, and $\boldsymbol{I}$ is the $P \times P$ identity matrix.

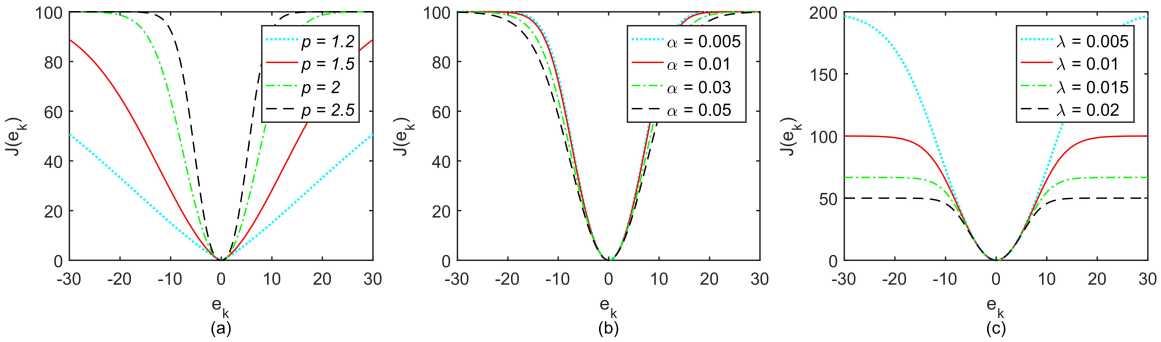

Fig. 2: Effects of different parameters on the ACHT cost function: (a) p; (b) α; and (c) λ.

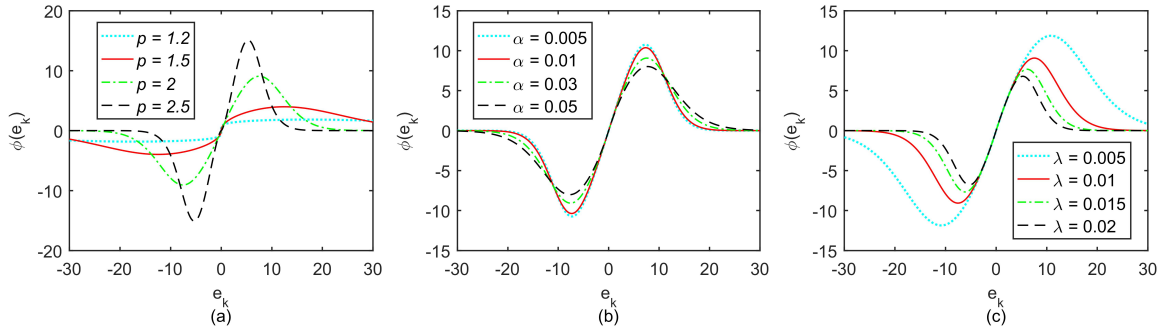

Fig. 3: Effects of different parameters on the derivative of the ACHT cost function: (a) p; (b) α; and (c) λ.

From the weight-update equation of the ACHT algorithm, the weight-error vector recursion is obtained as

$$\widetilde{\boldsymbol{w}}_{k+1} = \widetilde{\boldsymbol{w}}_k - \mu\varphi(e_k)\boldsymbol{x}_k. \tag{11}$$

Taking the squared Euclidean norm of both sides and then taking expectations yields

$$\begin{aligned}\mathrm{E}[\|\widetilde{\boldsymbol{w}}_{k+1}\|^2] = \mathrm{E}[\|\widetilde{\boldsymbol{w}}_k\|^2] - 2\mu\mathrm{E}[e_{a,k}\varphi(e_k)] \\ + \mu^2\mathrm{E}[\|\boldsymbol{x}_k\|^2\varphi^2(e_k)].\end{aligned} \tag{12}$$

At steady state, the weight-error energy converges to a constant, i.e.,

$$\lim_{k\to\infty} \mathrm{E}[\|\widetilde{\boldsymbol{w}}_{k+1}\|^2] = \lim_{k\to\infty} \mathrm{E}[\|\widetilde{\boldsymbol{w}}_k\|^2]. \tag{13}$$

Substituting the steady-state condition into the energy relation gives

$$2\lim_{k\to\infty} \mathrm{E}[e_{a,k}\varphi(e_k)] = \mu \lim_{k\to\infty} \mathrm{E}[\|\boldsymbol{x}_k\|^2\varphi^2(e_k)]. \tag{14}$$

To obtain the steady-state excess mean-square error (EMSE), the following two statistics are defined:

$$\begin{aligned} h_g &\triangleq \lim_{k\to\infty} \frac{\mathrm{E}[e_{a,k}\varphi(e_k)]}{\mathrm{E}[e_{a,k}^2]}, \\ h_u &\triangleq \lim_{k\to\infty} \mathrm{E}[\varphi^2(e_k)] \end{aligned} \tag{15}$$

where h_g characterizes the effective gain associated with the cross-correlation between the a priori error and the nonlinear score function, while h_u represents the steady-state mean-square value of the nonlinear score function.

The steady-state EMSE is defined as $\eta = \lim_{k\to\infty} \mathrm{E}[e_{a,k}^2]$. Under the small-step-size assumption, the a priori error $e_{a,k}$ is small compared with the measurement noise ξ_k. Using

$e_k = e_{a,k} + \xi_k$ and a first-order expansion of $\varphi(e_k)$ around ξ_k, we obtain

$$\begin{aligned}\lim_{k\to\infty} \mathrm{E}[e_{a,k}\varphi(e_k)] &\approx \eta\, \mathrm{E}[\varphi'(\xi_k)] \\ &= \frac{\mathrm{E}[\xi_k\varphi(\xi_k)]}{\sigma_\xi^2}\eta \\ &= h_g\eta\end{aligned} \tag{16}$$

The approximation follows from the small-step-size and independence assumptions, while the last equality follows from Gaussian integration by parts.

Using the fourth assumption and $\mathrm{E}[\|\boldsymbol{x}_k\|^2] = \mathrm{Tr}(\boldsymbol{R}) = P\sigma_x^2$, we obtain

$$\begin{aligned}\lim_{k\to\infty} \mathrm{E}[\|\boldsymbol{x}_k\|^2\varphi^2(e_k)] &\approx \mathrm{Tr}(\boldsymbol{R})h_u \\ &= P\sigma_x^2 h_u\end{aligned} \tag{17}$$

where $\mathrm{Tr}(\cdot)$ denotes the matrix trace.

Substituting the above expressions into the steady-state energy relation yields

$$\eta \approx \frac{\mu}{2}\frac{P\sigma_x^2 h_u}{h_g}. \tag{18}$$

The steady-state mean-square deviation (MSD) is defined as $\mathrm{MSD} = \lim_{k\to\infty}\mathrm{E}[\|\widetilde{\boldsymbol{w}}_k\|^2]$. For white input and under the standard independence approximation between $\boldsymbol{x}_k$ and $\widetilde{\boldsymbol{w}}_k$, we have

$$\begin{aligned}\eta &= \lim_{k\to\infty}\mathrm{E}[e_{a,k}^2] \\ &= \mathrm{E}\big[(\boldsymbol{x}_k^T\widetilde{\boldsymbol{w}}_k)^2\big] \\ &\approx \sigma_x^2\mathrm{E}[\|\widetilde{\boldsymbol{w}}_k\|^2] \\ &= \sigma_x^2\mathrm{MSD}.\end{aligned} \tag{19}$$

Therefore, the steady-state MSD of the ACHT algorithm is obtained as

$$\mathrm{MSD} \approx \frac{\mu P h_u}{2h_g}. \tag{20}$$

For numerical evaluation, the steady-state statistics are approximated by

$$\begin{aligned}h_g &\approx \frac{\mathrm{E}[\xi_k\varphi(\xi_k)]}{\sigma_\xi^2}, \\ h_u &\approx \mathrm{E}[\varphi^2(\xi_k)].\end{aligned} \tag{21}$$

If $\varphi(\xi_k)$ can be linearized near zero as $\varphi(\xi_k) \approx c\xi_k$, where $c = \varphi'(0)$ is the local linear coefficient, then $h_g \approx c$, $h_u \approx c^2\sigma_\xi^2$, and hence

$$\begin{aligned}\eta &\approx \frac{\mu}{2}P\sigma_x^2 c\sigma_\xi^2, \\ \mathrm{MSD} &\approx \frac{\mu}{2}Pc\sigma_\xi^2.\end{aligned} \tag{22}$$

For $p = 2$, the nonlinear score function is locally linear with $\varphi'(0) = 2$. When the measurement noise is sufficiently concentrated in this linear region, the steady-state MSD can be further approximated as $\mathrm{MSD} \approx \mu P\sigma_\xi^2$. This result is consistent with the steady-state performance form of the conventional LMS algorithm, indicating that the ACHT algorithm has linear update characteristics similar to LMS in the small-error region, while improving robustness in large-error environments through the nonlinear compression mechanism.

3.2 Computational Complexity

Following the computational complexity analysis in [12], Table 1 compares the computational complexity of ACHT with that of the existing algorithms. Although ACHT requires additional scalar operations, its computational complexity remains linear in the filter length L.

Table 1: Computational complexity of related adaptive filtering algorithms

Algorithms	×	+	sign	÷
LMS	$2L+1$	$2L$	–	–
GMCC	$2L+4$	$2L$	1	–
MVC	$2L+4$	$2L+1$	1	1
LHCAF	$2L+2$	$2L$	–	–
ATLMS	$2L+4$	$2L+1$	–	1
ACHT	$2L+8$	$2L+2$	–	2

4 Computer Simulations

To evaluate the steady-state performance and robustness of the proposed ACHT algorithm, system identification simulations are conducted under different noise conditions. Both the

unknown system and the adaptive filter have a length of $L = 128$. The input signal is generated using randn(1,N), corresponding to zero-mean white Gaussian noise with unit variance ($\sigma_x^2 = 1$). All adaptive filters are initialized with $\boldsymbol{w}_0 = 0$, and the results are averaged over 200 independent Monte Carlo trials.

The theoretical steady-state performance is verified under Gaussian measurement noise, while parameter sensitivity and algorithm comparisons are evaluated under impulsive noise conditions.

The normalized mean square deviation (NMSD) is used to evaluate convergence performance and is defined as

$$\mathrm{NMSD}_k = \mathrm{E}\left[\frac{\|\boldsymbol{w}^o - \boldsymbol{w}_k\|^2}{\|\boldsymbol{w}^o\|^2}\right]. \tag{23}$$

The results are expressed in decibels as $10\log_{10}(\mathrm{NMSD}_k)$.

4.1 Theoretical Verification of Steady-State Performance

To verify the steady-state analysis in Section 3, the theoretical NMSD is compared with Monte Carlo simulation results under zero-mean white Gaussian measurement noise $v_k = \xi_k$ with variance $\sigma_\xi^2 = 0.01$.

The ACHT parameters are set to $p = 2$, $\alpha = 0.1$, and $\lambda = 0.03$. By varying the step size μ, the theoretical and simulated steady-state NMSD values are obtained for comparison.

Fig. 4 shows that the theoretical and simulated steady-state NMSD values agree closely, particularly for small step sizes ($\mu < 0.002$). As μ increases, the steady-state NMSD also increases, with slight differences between the theoretical and simulated results at larger step sizes.

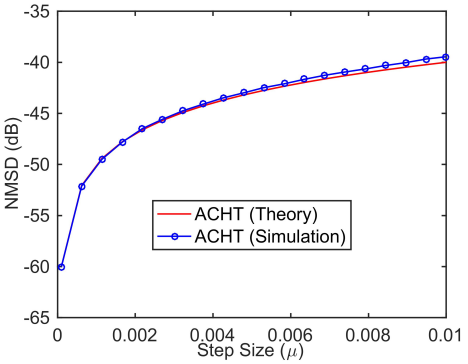

Fig. 4: Theoretical and simulated steady-state NMSD for different step sizes.

4.2 Parameter Sensitivity Analysis

To investigate the convergence performance of the ACHT algorithm under impulsive interference, the Bernoulli–Gaussian (BG) impulsive noise model is adopted. The measurement noise is expressed as

$$v_k = \xi_k + \omega_k n_k \tag{24}$$

where ξ_k denotes the background noise, ω_k is a Bernoulli random variable, and n_k is zero-mean Gaussian impulsive noise with variance σ_n^2. The random variables ξ_k, ω_k, and n_k are mutually independent.

In this subsection, the background noise is zero-mean white Gaussian noise with variance $\sigma_\xi^2 = 0.01$. The impulse occurrence probability is set to $P(\omega_k = 1) = P_r = 0.1$, and the impulsive-noise variance is set to $\sigma_n^2 = 1000\,\mathrm{Var}(\boldsymbol{x}_k^{\mathrm{T}}\boldsymbol{w}^o)$.

The step size is fixed at $\mu = 0.001$. Only one parameter is varied at a time, while the others are held constant. Fig. 5 shows the corresponding NMSD learning curves.

Fig. 5(a) shows the effect of p, with $\alpha = 0.1$ and $\lambda = 0.03$ fixed. The tested values are $p = 1.2$, 1.5, 2, and 2.5. As p increases from 1.2 to 2, convergence becomes faster and the steady-state NMSD decreases. At $p = 2.5$, both convergence speed and steady-state accuracy are slightly worse than those at $p = 2$.

Fig. 5(b) shows the effect of α, with $p = 2$ and $\lambda = 0.03$ fixed. The tested values are $\alpha = 0.05$, 0.1, 0.2, and 0.3. Increasing α slightly slows convergence and reduces the steady-state NMSD, although the differences among the curves are small.

Fig. 5(c) shows the effect of λ, with $p = 2$ and $\alpha = 0.1$ fixed. The tested values are $\lambda = 0.01$, 0.02, 0.03, and 0.04. A larger λ leads to slower convergence but a lower steady-state NMSD. The lowest steady-state NMSD is obtained at $\lambda = 0.04$, at the cost of more iterations.

Considering both convergence speed and steady-state accuracy, $p = 2$, $\alpha = 0.1$, and

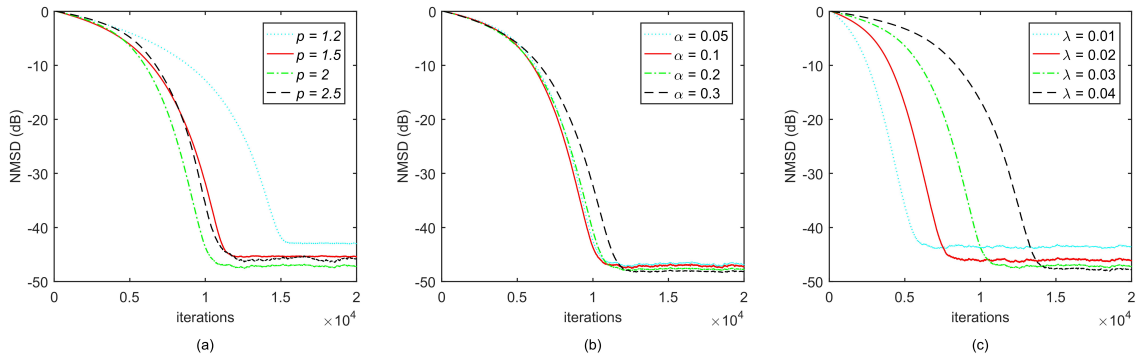

Fig. 5: Effects of different parameters on the NMSD learning curves of the ACHT algorithm: (a) p; (b) α; and (c) λ.

$\lambda = 0.03$ are used in the subsequent algorithm comparisons.

4.3 Comparative Simulations of Multiple Algorithms

To further evaluate the robustness of ACHT algorithm under different noise conditions, its performance is compared with five adaptive filtering algorithms, namely LMS, GMCC, MVC, LHCAF, and ATLMS. All algorithms are evaluated under the same conditions in each experiment, with their parameter settings summarized in Table 2.

Table 2: Parameter settings of the compared algorithms

Algorithm	Parameter Settings
LMS	$\mu = 0.001$
GMCC	$\mu = 0.001, \lambda = 0.01, \alpha = 2$
MVC	$\mu = 0.0012, p = 2, \lambda = 0.01$
LHCAF	$\mu = 0.0015, \lambda = 3$
ATLMS	$\mu = 0.0015, \lambda = 0.03$
ACHT	$\mu = 0.001, p = 2, \lambda = 0.03, \alpha = 0.1$

The BG impulsive noise model introduced in Section 4.2 is retained. Four background noise distributions are considered: zero-mean Laplacian noise with a variance of 0.01; zero-mean Gaussian noise with a variance of 0.01; uniform noise distributed over $[-\sqrt{0.01}, \sqrt{0.01}]$; and binary noise taking values of -1 and 1 with equal probability.

Fig. 6 presents the NMSD learning curves of the compared algorithms under the four noise conditions. As shown in Fig. 6, the conventional LMS algorithm is highly sensitive to impulsive disturbances, resulting in degraded steady-state performance. GMCC, MVC, LHCAF, and ATLMS alleviate the influence of large-amplitude errors to varying degrees, but exhibit differences in convergence speed and steady-state accuracy. In comparison, the proposed ACHT algorithm achieves favorable convergence performance and low steady-state NMSD across the considered noise environments, demonstrating its robustness against impulsive noise.

5 Conclusion

This paper proposes an ACHT algorithm for robust adaptive filtering under the considered noise conditions. By combining adaptive compression with hyperbolic-tangent saturation mapping, ACHT reduces the influence of large-amplitude outliers on weight updates. Approximate steady-state EMSE and MSD expressions are derived based on the energy conservation relation and validated through Monte Carlo simulations. The results indicate that ACHT achieves low steady-state NMSD and competitive convergence performance under the tested conditions. Future work will extend the theoretical analysis to non-Gaussian impulsive noise and investigate the algorithm under correlated inputs.

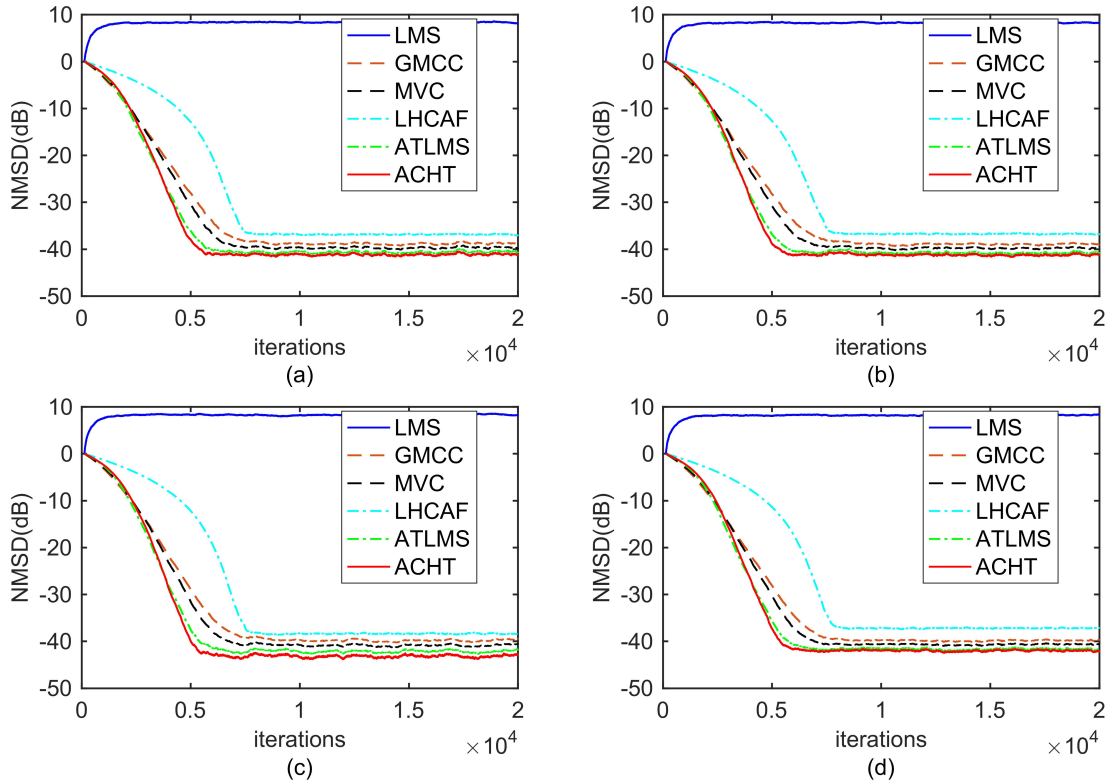

Fig. 6: NMSD learning curves of LMS, GMCC, MVC, LHCAF, ATLMS, and ACHT under different noise conditions: (a) Laplacian noise; (b) Gaussian noise; (c) uniform noise; and (d) binary noise.

Declarations

Conflict of interest The authors declare that they have no conflict of interest.

Funding This work was supported by National Natural Science Foundation of China (Grant: 62201097, 62501002).

Data availability Data are available from the corresponding author on reasonable request.

References

[1] Sayin, M.O., Vanli, N.D., Kozat, S.S.: A novel family of adaptive filtering algorithms based on the logarithmic cost. IEEE Transactions on Signal Processing **62**, 4411–4424 (2014) https://doi.org/10.1109/TSP.2014.2333559

[2] Chen, B., Xing, L., Zhao, H., Zheng, N., Príncipe, J.C.: Generalized correntropy for robust adaptive filtering. IEEE Transactions on Signal Processing **64**, 3376–3387 (2016) https://doi.org/10.1109/TSP.2016.2539127

[3] Huang, F., Zhang, J., Zhang, S.: Maximum versoria criterion-based robust adaptive filtering algorithm. IEEE Transactions on Circuits and Systems II: Express Briefs **64**, 1252–1256 (2017) https://doi.org/10.1109/TCSII.2017.2671521

[4] Huang, F., Zhang, J., Zhang, S.: A family of robust adaptive filtering algorithms based on sigmoid cost. Signal Processing **149**, 179–192 (2018) https://doi.org/10.1016/j.sigpro.2018.03.013

[5] Liu, C., Jiang, M.: Robust adaptive filter with lncosh cost. Signal Processing **168**, 107348 (2020) https://doi.org/10.1016/j.sigpro.2019.107348

[6] Wang, S., Wang, W., Xiong, K., Iu, H.H.C., Tse, C.K.: Logarithmic hyperbolic cosine adaptive filter and its performance analysis. IEEE Transactions on Systems, Man, and Cybernetics: Systems **51**, 2512–2524 (2021) https://doi.org/10.1109/TSMC.2019.2915663

[7] Huo, Y., Long, X., Lian, P., Wang, D.: A kind of versoria function normalized adaptive filtering algorithm. Journal of Electronics and Information Technology **43**, 335–340 (2021) https://doi.org/10.11999/JEIT191003

[8] Lu, M., Peng, S., Chen, B.: Convex combination of multiple adaptive filters under the maximum correntropy criterion. Journal of Electronics and Information Technology **43**, 263–269 (2021) https://doi.org/10.11999/JEIT200288

[9] Kumar, K., Karthik, M.L.N.S., George, N.V.: A novel family of sparsity-aware robust adaptive filters based on a logistic distance metric. IEEE Transactions on Signal Processing **70**, 6128–6141 (2022) https://doi.org/10.1109/TSP.2022.3233528

[10] Wang, B., Li, H., Gao, S., Zhang, M., Xu, C.: A variable step size least mean p-power adaptive filtering algorithm. Journal of Electronics and Information Technology **44**, 661–667 (2022) https://doi.org/10.11999/JEIT210073

[11] Jia, W., Kong, S., Cai, T., Li, M., Jin, Y., Wang, P., Dai, Z.: Steady-state performance analysis of the arctangent lms algorithm with gaussian input. IEEE Transactions on Circuits and Systems II: Express Briefs **70**, 3189–3193 (2023) https://doi.org/10.1109/TCSII.2023.3248222

[12] Abdelrhman, O.M., Dou, Y., Li, S.: A generalized robust logarithmic family-based adaptive filtering algorithms. IEEE Transactions on Circuits and Systems II: Express Briefs **70**, 3199–3203 (2023) https://doi.org/10.1109/TCSII.2023.3246235

[13] Patel, V., Bhattacharjee, S.S., Christensen, M.G.: Generalized soft-root-sign based robust sparsity-aware adaptive filters. IEEE Signal Processing Letters **30**, 200–204 (2023) https://doi.org/10.1109/LSP.2023.3252412

[14] Song, P., Zhao, H., Luo, L., Yang, S.: Least mean square algorithm based on hyperbolic tangent function framework. Journal of Signal Processing **39**, 2030–2036 (2023) https://doi.org/10.16798/j.issn.1003-0530.2023.11.012

[15] Huo, Y., Xu, T., Qi, Y., *et al.*: A family of robust diffusion adaptive filtering algorithms based on the tanh framework. Circuits, Systems, and Signal Processing **43**, 1938–1956 (2024) https://doi.org/10.1007/s00034-023-02552-7

[16] Liu, Q., He, Y.: Quaternion hyperbolic tangent geman–mcclure for adaptive filtering. IEEE Transactions on Circuits and Systems II: Express Briefs **71**, 3618–3622 (2024) https://doi.org/10.1109/TCSII.2024.3364503

[17] Jain, S., Kumar, P., Mitra, R., Singya, P.K., Sharma, S., Bhatia, V.: Generalized versoria soft-root-sign-based adaptive filter for system identification under impulsive noise. IEEE Access **13**, 179315–179332 (2025) https://doi.org/10.1109/ACCESS.2025.3622203

[18] Li, G., Zhang, H., Wang, S., Wang, G., Zhao, J.: Generalized mixed-norm maximum correntropy for robust adaptive filtering. Applied Acoustics **228**, 110382 (2025) https://doi.org/10.1016/j.apacoust.2024.110382

[19] Guo, W., Liao, R., Zhi, Y., Liao, G.: Robust adaptive filtering for heavy-tailed noise and colored noise via lncosh-generalized hyperbolic secant. IEEE Transactions on Aerospace and Electronic Systems **61**, 17238–17251 (2025) https://doi.org/10.1109/TAES.2025.3603797